Hydro-mechanical upscaling of a fractured rockmass using a 3D numerical approach

Alain Thoraval, Vincent Renaud

HYDRO-MECHANICAL UPSCALING OF A FRACTURED ROCKMASS USING A 3D NUMERICAL APPROACH

Thoraval Alain, Renaud Vincent
INERIS, ENSMN, Parc de Saurupt, 54042 Nancy Cedex, France.

Abstract: A new upscaling method has been developed using 3D numerical tools (RESOBLOK & 3DEC). This method has been successfully compared with standard analytical approaches in the case of a simple fracture network. This method has been applied to determine the equivalent permeability, stiffness and Biot tensor of a real fracture rock-mass at different scales. The effects of the fracture network properties and of the state of stress on the result have been investigated.

1. CONTEXT OF THE WORK AND OBJECTIVES

This work is part of the INERIS contribution to work package 3 (WP3) of the European project BENCHPAR. The purpose of WP3 is the better understanding the impact of upscaling on the THM processes on Performance Assessment of nuclear waste disposal problems.

The INERIS contribution to WP3 consist in:

- The development and evaluation of a new upscaling method, and its application to WP3 fracture data;
- Comparison between H, HM, THM simulations considering an equivalent homogeneous medium with FLAC3D (whose properties will have been determined previously by the upscaling process).

This paper presents only the upscaling work.

2. DESCRIPTION OF THE UPSCALING APPROACH & VERIFICATIONS

A new upscaling method has been proposed by INERIS to determine the equivalent hydro mechanical properties of a fractured rock-mass. This method is based on the 3D numerical simulations of the behaviour of a "sample" of fractured rock-mass submitted to different hydromechanical boundary conditions. The simulations are defined in order to determine the equivalent permeability, stiffness and Biot tensor of a fractured rock-mass.

Two numerical tools are used: RESOBLOK [Heliot, 1988] to generate the 3D fracture network; 3DEC [Itasca Consulting Group, 1994; Damjanac, 1994] to make the hydro-mechanical computations.

2.1 Generation of the fracture network

The code used to generate the fracture network (RESOBLOK) is based on the assumption that the fracture can be considered as polygon. This code is able to make determinist or stochastic simulations. To make the stochastic simulations done for the WP3 exercise (figure 1), the following assumptions are done:

- Fracture density (number of fracture per unit volume of rock - P_{31}) is assumed to follow a Poisson law;
- Fracture orientation is assumed to follow a Fisher law. Average dip & dip direction as well as the Fisher coefficient (k_f) has to be given for the different fracture sets;
- Fracture length is assumed to follow a power law distribution of the form $N=CL^{-D}$, where N is the number of fractures which are equal to or greater than a given trace length L, D is the fractal dimension and C is a constant.

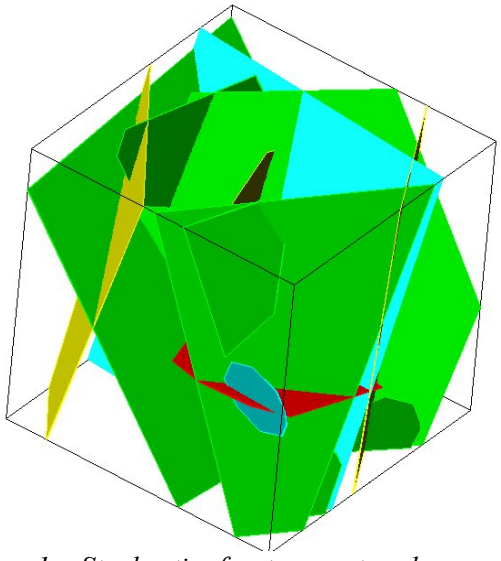

Figure 1. Stochastic fracture network generated by RESOBLOK.

2.2 Determination of the equivalent permeability tensor Kij

The hydraulic gradient J and the fluid flow Q are linked by the relationship:

$$Qi = -Kij\ Jj \qquad (1)$$

To determine all the tensor terms with 3DEC, 3 sets of (hydraulic) boundary conditions have to be defined (figure 2).

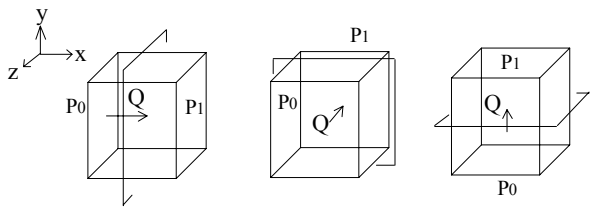

Figure 2. Boundary conditions used to determine the permeability tensor with 3DEC.

After each computation, the "equivalent" vectorial flowrate is averaged from the flowrate value at different locations of the fracture network. The different terms of the equivalent permeability tensor are then computed from equation (1).

The results of this new upscaling approach have been compared with an analytical solution given for the simple geometry (figure 3).

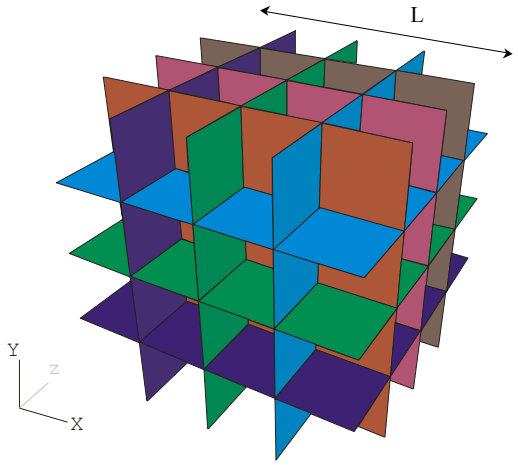

Figure 3. Fracture network used for comparison with analytical upscaling approach.

The analytical equivalent hydraulic conductivity tensor can be expressed in this case as following:

$$K_{ij\ analytical} = (\rho\ g\ a^3 / 2\ \mu\ L)\ \delta_{ij} \qquad (2)$$

$$= 2.45\ 10^{-7}\ m/s$$

where: a (= 10^{-4} m) is the hydraulic aperture of the fracture; μ (= 10^{-3} Pa s) is the dynamic viscosity of the fluid; (L = 20 m) is the edge length of the model; ρ = 1000 kg/m^3; g =9.81 m/s^2.

The equivalent permeability given by 3DEC is:

$$K_{ij\ 3DEC} = (6\ \rho\ g\ a\ q_{3DEC} / \Delta P)\ \delta_{ij} \qquad (3)$$

$$= 2.35\ 10^{-7}\ m/s$$

where q_{3DEC} = 4 10^{-2} m/s is the discharge (m/s) computed with 3DEC for ΔP = 10^6 Pa.

We can see that the 3DEC result is very close to the analytical solution.

2.3 Determination of the equivalent Stiffness tensor Tijkl

The stress tensor σ_{ij}, the elastic strain tensor ε_{kl}, the Biot's tensor B_{ij} and the Biot coefficient G are linked by the Biot's equation:

$$\sigma_{ij} = T_{ijkl}\ \varepsilon_{kl} - B_{ij}\ P \qquad (4)$$

$$P = -G(B_{kl}\ \varepsilon_{kl} - \xi) \qquad (5)$$

where P is the fluid pressure and ξ the fluid production.

To determine all the tensor terms with 3DEC, 6 sets of (mechanical) boundary conditions have to be defined (Figure 4 and 5).

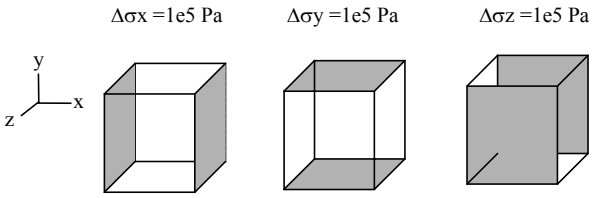

An initial state of stress (σ = 1e6 Pa) is applied into the model; a constant stress increment (Δσ = 1e5 Pa) is apply on the grey faces

Figure 4. First set of boundary conditions used to determine Tijkl with 3DEC.

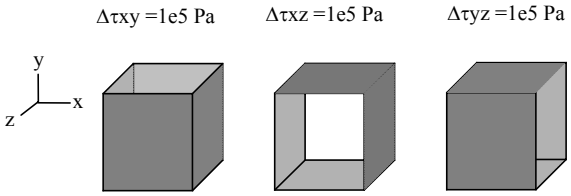

An initial state of stress (σ = 1e6 Pa) is applied into the model; a constant shear stress increment (Δτ = 1e5 Pa) is apply on the grey faces

Figure 5. Second set of boundary conditions used to determine Tijkl with 3DEC.

During each 3DEC runs, the average strain tensor is computed from displacement differences between opposite face of the model (100 pairs of point is used for each strain term).

A verification has been done again for the same simple geometry (figure 3). From Oda theory [1986], it can be shown that, in this case, $(T_{ijkl})^{-1}$ is equal to:

$$\begin{bmatrix} \frac{1}{E}+\frac{n}{LK_n} & -\frac{\nu}{E} & -\frac{\nu}{E} & 0 & 0 & 0 \\ -\frac{\nu}{E} & \frac{1}{E}+\frac{n}{LK_n} & -\frac{\nu}{E} & 0 & 0 & 0 \\ -\frac{\nu}{E} & -\frac{\nu}{E} & \frac{1}{E}+\frac{n}{LK_n} & 0 & 0 & 0 \\ 0 & 0 & 0 & \frac{1+\nu}{E}+\frac{n}{LK_s} & 0 & 0 \\ 0 & 0 & 0 & 0 & \frac{1+\nu}{E}+\frac{n}{LK_s} & 0 \\ 0 & 0 & 0 & 0 & 0 & \frac{1+\nu}{E}+\frac{n}{LK_s} \end{bmatrix}$$

Assuming E (Young's modulus)=5.294 GPa; ν (Poisson ratio) =0.324; Kn & Ks (normal &shear joint stiffness) =1 GPa/m; n (number of fracture in each fracture set) = 3; L = 20 m, we get (in GPa):

$$Tijkl_{\,analytical} = 3.205 \begin{bmatrix} 1 & 0.220 & 0.220 & 0 & 0 & 0 \\ 0.220 & 1 & 0.220 & 0 & 0 & 0 \\ 0.220 & 0.220 & 1 & 0 & 0 & 0 \\ 0 & 0 & 0 & 0.780 & 0 & 0 \\ 0 & 0 & 0 & 0 & 0.780 & 0 \\ 0 & 0 & 0 & 0 & 0 & 0.780 \end{bmatrix}$$

The determination of this matrix with the numerical approach gives the following result:

$$Tijkl_{\,3DEC} = 3.205 \begin{bmatrix} 1.000 & 0.220 & 0.220 & -0.014 & -0.014 & -0.005 \\ 0.220 & 1.000 & 0.220 & -0.014 & -0.005 & -0.014 \\ 0.220 & 0.220 & 1.000 & -0.005 & -0.014 & -0.014 \\ -0.001 & -0.002 & 0.000 & 0.780 & 0.000 & 0.000 \\ 0.001 & 0.000 & 0.000 & 0.000 & 0.780 & 0.000 \\ 0.001 & 0.003 & 0.003 & 0.000 & 0.000 & 0.780 \end{bmatrix}$$

It can be noticed that, in all cases, the differences between the analytical and the 3DEC solution are very small (less than 1.5%).

2.4 Determination of the equivalent Biot tensor Bij

The numerical procedure is to impose a fluid pressure built up from P to P + ΔP within the model, assuming no mechanical deformation at the boundaries. In this case the Biot's equations (4 & 5) can be rewritten as follows:

$$\Delta\sigma_{ij} = - B_{ij}\,\Delta P \;\;\&\;\; \Delta P = G\,\Delta\xi. \qquad (6)$$

with $\Delta\xi = V_1\text{-}V_0/V_t$, where V_0 the initial fluid volume (under P), V_1 is the final fluid volume (under P+ΔP) and V_t the total model volume.

For the geometry of figure 3, it can be shown:

$$B_{ij} = \frac{nE}{LK_n(1-2\nu)+nE}\,\delta_{ij} \quad and \quad G = \frac{LK_n}{3n\delta_{ij}(\delta_{ij}-B_{ij})} \qquad (7)$$

With 3DEC, we determine the average stress variation $\Delta\sigma_{ij}$ and volumetric water content variation $\Delta\xi$ induced by the hydraulic pressure ΔP.

We have found again in this case that the difference between analytical and numerical solution are below 2%.

3. APPLICATION OF THE UPSCALING TECHNIQUE TO WP3

The objective of this section is to compute, with the numerical approach already presented and validated, the equivalent permeability tensor of the fracture network of the WP3 case. The set of computation presented here concerned the fracture network of formation 1 (computation has also been done for formation 2 and the fault zone).

The size of the zone of interest where the fracture network is simulated has been progressively increased from 2 m to the greater possible size according to the numerical problem encountered. Five simulations have been done for each model size to get an idea of the standard deviation.

3.1 Input of the fracture network geometry into 3DEC

3.1.1 RESOBLOK simulations

The fracture network is generated by RESOBLOK from the data gathered in Table 1.

Table 1: Joint set properties for formation 1

Fracture set	dip (°)	dd (°)	k_f	P_{11} density (FLT = 0.5 m)	D
1	8	145	5.9	0.16	1.2
2	88	148	9	0.31	0.7
3	76	21	10	1.0	1.1
4	69	87	10	0.5	1.1

The simulations have been done considering initial value of P_{31} equal to the value of P_{11} (for a Fracture Length Threshold of 0.5 m) given in Table 1. Average values of P_{22}, computed from several RESOBLOK simulations, were compared to P_{22} measurements ($5m/m^2$ for a fracture length threshold of 0.5 m) to evaluate the realism of the simulations. The results are gathered in Table 2.

We can notice that the computed P_{22} value at 3 m or 4 m are close to the measured value (5m/m2).

Table 2: Determination of fracture density from RESOBLOK fracture network simulations.

«Sample » size	Set	Computed P22 density (m/m^2)
3×3×3 m3	1	0.11
	2	1.37
	3	1.87
	4	0.97
	Total	**4.39**
4×4×4 m^3	1	0.26
	2	1.27
	3	2.57
	4	0.97
	Total	**5.01**

3.1.2 Interfacing RESOBLOK to 3DEC

A specific command of RESOBLOK is used to generate a 3DEC file including all information regarding fracture network geometry.

3DEC does not allow generating fractures that stop inside a block. During the 3DEC cutting process, the plane where the RESOBLOK polygonal fracture is lying is continued up to the next fracture (or block face). However, 3DEC automatically distinguish 2 zones (from information output from RESOBLOK): an "active" zone inside the polygon area (real joint), an "inactive" zone outside the polygon (fictitious joint). So 3DEC is able to "give" different properties to "real" joint and fictitious joint.

3.1.3 Checking the effect of fictitious joints on the equivalent permeabity tensor

We have shown, from various 3DEC runs, that the prolongation of joint up to the next block face (that artificially increased the fracture network connectivity) could lead to overestimate the permeability by a factor of 2 or 3.

The hydraulic aperture used for the real joint is supposed to be 6.5 10^{-5} m. We have considered a hydraulic aperture of 10^{-6} m for the fictitious joint. We have checked that the equivalent hydraulic permeability tensor computed considering a fictitious joint network is 5 orders of magnitude smaller than if we consider a real joint network.

3.1.4 Checking the effect of fictitious joints on the equivalent stiffness tensor

The joint stiffness used for the real joint is supposed to be 4.34 10^{-11} Pa/m. We have considered a joint stiffness of 10^{-12} Pa/m for the fictitious joint. We have checked that, for this value, the equivalent stiffness tensor is very close to the intact rock stiffness tensor.

We have evaluated the effect of considering the fictitious joints as real joints on the equivalent stiffness tensor T_{ijkl}. We can notice that the terms of the equivalent stiffness tensor terms are smaller if we consider 3DEC fictitious joints are real. For the WP3 case (where high joint stiffness values are considered) the differences remain small. It increased up to 30 % for Kn = 4.34 10^{-10} Pa/m.

3.1.5 Limitation of 3DEC code

We have noticed that some problems occur during the cutting process into 3DEC (version 3.00.073), when the fracture number becomes important (and maybe when the angle between fracture become small). I happens that in some cases, the cutting is rejected or an error appears later in the process of block geometry recognition. Some efforts have been done (in collaboration with ITASCA) to overcome those limitations but, up to now, no satisfying answer has been found

The consequence of this limitation is that the determination of K_{ij} and T_{ijkl} was not possible (for WP3 data) for a model size higher than 2×2×2 m^3 if we want to avoid artificial prolongation of joint into 3DEC. The limit is push back to 5×5×5 m^3 for T_{ijkl} (and unchanged for K_{ij}) a artificial joint prolongation is considered.

3.2 Determination of the WP3 "equivalent" permeability tensors (Kij)

3.2.1 Assuming constant hydraulic aperture

We have assumed that the hydraulic apertures were constant and equal to 6,5 10^{-5} m. The equivalent permeability tensor is given below at 2 m scale for the fracture network of formation 1 and considering a fracture length threshold of 0.5 m:

$$K_{ij} = \begin{bmatrix} 5.06 & -0.44 & 0.25 \\ -0.54 & 6.95 & -0.40 \\ 0.36 & -0.19 & 4.53 \end{bmatrix} \pm \begin{bmatrix} 1.65 & 0.62 & 0.52 \\ 0.81 & 1.88 & 0.62 \\ 0.33 & 0.56 & 1.60 \end{bmatrix} (10^{-8} \text{ m/s})$$

Because of 3DEC limitations, the upcaling was done only at 2 m scale; so the existence of a REV (and its value) could not be established at the present time.

Fracture network simulations were done considering the relation (established from

measurements by Nirex (Andersson, 2000) between the number of fractures per meter and the fracture length threshold. With a view to the fracture network simplification, we have tried to determine the effect of the fracture length threshold (used to make the RESOBLOK simulations) on the upscaling process. Unfortunately, we have shown that, at 2 m scale, it was not possible to conclude about the effect of the fracture length threshold on K_{ij}. The reason is that the connection of the fracture network to the model boundaries, where the pressure gradient is applied, is artificially increased when the model size is small in comparison with the fracture length threshold.

3.2.2 Assuming stress dependent hydraulic aperture

For HM computation, 3DEC consider a relation between the hydraulic aperture "a" and the mechanical aperture "u" that can be written: $a = a_0 + \Delta u$, where a_0 is the zero stress aperture. A maximum and residual aperture is considered for numerical stability reason. We have assumed that $a_{max} = a_0 = 6.5\ 10^{-5}$ m and that $a_{res} = 1.8\ 10^{-5}$ m.
Figure 6 represent the evolution of the diagonal terms of the equivalent permeability tensor with stress applied on the model boundaries (at 2 m scale).

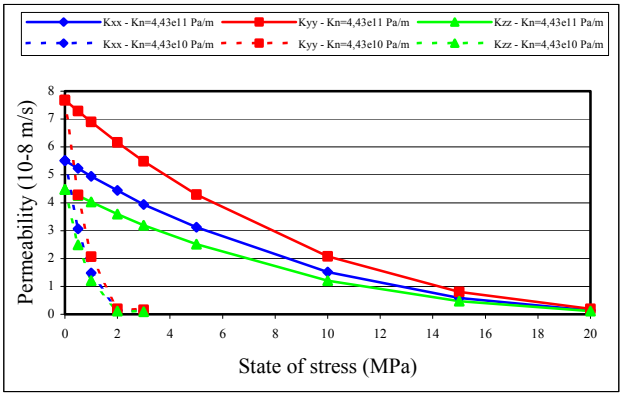

Figure 6 Equivalent permeability tensor variation with stress.

We can see a decreasing of the permeability when the applied stress increases. This decreasing is much faster if the normal joint stiffness is assumed to be smaller ($4.43\ 10^{10}$ Pa/m instead of $4.43\ 10^{11}$ Pa/m). It can be notice that there is a residual equivalent permeability (around 10^{-9} m/s) that has to be related to the residual hydraulic aperture. That residual permeability is reached for $\sigma > 20$ MPa (≈ 800 m) if the joint normal stiffness is $Kn = 4.43\ 10^{11}$ Pa/m and for $\sigma > 2$ MPa (≈ 80 m) $Kn = 4.43\ 10^{10}$ Pa/m.

In this work we have assumed no relation between the joint stiffness and the stress or with the fracture length. This assumption could be revisited later on. We have also considered an isotropic state of stress. Others stress conditions could be applied and would probably involve other kinds of evolution of the equivalent permeability tensor.

3.2 Determination of the WP3 "equivalent" stiffness tensor (T_{ijkl})

T_{ijkl} has been first determined considering a prolongation of the joint up to the next joint (all the cutting plane generated by 3DEC are assumed to be active). The results for formation 1 are gathered in Table 3 (we have distinguish the average values from the standard deviation of the different terms).

Table 3: Equivalent stiffness tensor for formation 1 at 2 m scale

a – average values

67,12	15,71	13,44	-4,61	-2,54	-0,91
15,73	72,86	14,38	-5,13	-1,08	-2,51
13,38	14,41	60,97	-1,49	-2,32	-2,75
-1,97	-2,07	-0,60	54,50	-0,79	-0,89
-1,51	-0,44	-1,25	-1,17	49,99	-0,66
-0,46	-1,55	-1,21	-0,77	-1,38	52,00

5,77	2,70	1,71	4,69	3,47	1,35
2,66	7,58	2,10	5,21	1,68	3,76
1,75	2,17	4,42	1,62	3,04	3,74
2,25	2,52	0,75	3,56	1,06	1,06
1,55	0,58	1,38	0,99	2,06	1,52
0,61	1,95	1,65	1,12	1,34	2,73

b- standart deviation

Figure 7 and figure 8 gives the evolution of the average value and standard deviation of the diagonal terms of T_{ijkl} terms from 2 m to 5 m scale.

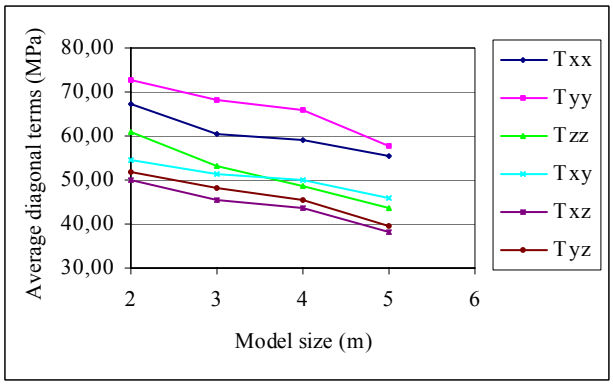

Figure 7. Evolution of average T_{ijkl} diagonal terms for formation 1.

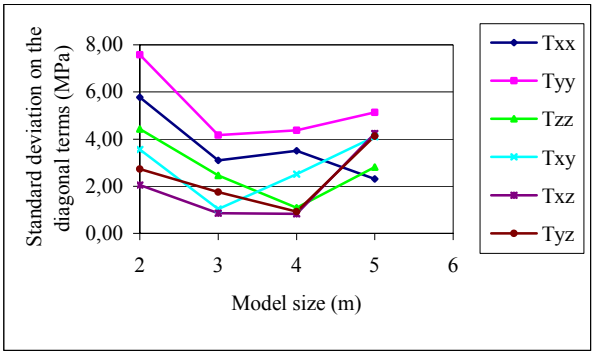

Figure 8. Evolution of standard deviation on T_{ijkl} diagonal terms for formation 1.

From this result, we can see that the REV is higher than 5 m. Model sizes become too important (≈ 250 Mo) to allow us to check if stabilization is about to be reached.

T_{ijkl} has also been determined at 2 m scale considering the real length of the joint. Differences with the previous simulation remain below 10 %. This could lead us to think that this factor is not very important for the equivalent mechanical behaviour. This result is consistent with the fact that no significant fracture length threshold effect has been shown on T_{ijkl}.

The results is highly related to the choice of the fracture stiffness value. This invites us to investigate later on the effect of stress on the result considering stress dependent stiffness.

4. CONCLUSIONS

An upscaling approach based on the 3D numerical simulation has been set up. Very good correlations with analytical solutions have been found for a network made of 3 sets of parallel fractures.

This approach has then been applied to fracture data given in the WP3 specifications in order to get the equivalent hydromechanical properties of the fractured rockmass.

The equivalent permeability tensor K_{ij} has been computed at 2 m scale considering the real length of the joint (we have shown the importance to avoid artificial joint prolongations). The REV could not be estimated due to code limitation reasons. The relation between permeability and stress (considering an isotropic state of stress) has been determined and is highly dependent on the joint stiffness value.

The equivalent stiffness tensor T_{ijkl} has been computed up to 5 m scale. No clear conclusion can be given for the mechanical REV. We have notice that the fracture network connectivity does not seem to have a strong influence on T_{ijkl}.

The new method presented in this paper is challenging because it is based on 3D explicit simulations of the hydromechanical behaviour of a fractured rock-mass. Some improvements are still to be done to make this method really operational. However those 3D results could contribute (through comparisons) to the evaluation of the more operational 2D methods used in BENCHPAR WP3. Accordingly this contribution could be profitable to the upscaling world.

5. ACKNOWLEDGEMENT

We wish to thank Ki-Bok Min from Royal Institute of Technology (KTH), Sweden for a helpful collaboration about mechanical upscaling using UDEC and 3DEC, and Johan Andersson from JA Streamflow AB, Sweden for many fruitful advices. We acknowledge with gratitude the financial support of the European Community and of the MEDD and MEFI french ministries.

6. REFERENCES

Damjanac, B. 1994. *A three-dimensional numerical model of water flow in a fractured rock mass*. Doctoral Thesis proposal, March 1994, University of Minnesota.

Heliot, D. 1988. *Generating a Blocky Rock Mass*. Int. J. Rock. Mini Sci & Geomech. Abstr. Vol 25, N°3 pp 127-138, 188.

Itasca Consulting Group, Inc., 1994. *3DEC 3-Dimensional Distinct Element Code*. Minneapolis, Minnesota: ICG.

Oda, 1986. *A equivalent continuum model for coupled stress and fluid flow analysis in joint rock masses*. Water Ressources Research, 22, pp 1845-1856.

Andersson, J. 2000. *Understanding the impact of upscaling THM processes on performance assessment.* version 6 (08/12/2000).

Vuillot, E. 1995. *Modélisation thermo-hydro-mécanique de massifs rocheux fracturés. Application au stockage de déchets radioactifs*. Thèse de Doctorat de l'INPL, Nancy, France.